

Trends in Immunotherapy

https://ojs.ukscip.com/index.php/ti

Article

Orchestrating Tumor Microenvironment Modulation Through Artificial Intelligence-Driven Nanoparticle Systems for Precision Cancer Therapeutics

S. Sivanandam 1* , Mohammad Givi Efgivia 2 , Ashok K 3 , S Manikandan 4 , C.S. Preetham Reddy 5 , Ykuntam Yamini Devi 6

Received: 30 May 2025; Revised: 19 June 2025; Accepted: 27 June 2025; Published: 31 October 2025

Abstract: The tumor microenvironment (TME) is an environment that affects the growth, progression, and resistance of the tumor. AI is already transformational in the process of comprehending and attacking the TME. Using datasets with many more variables and different aspects, AI models can predict tumor behavior with greater precision than conventional techniques. In this work, the polyethylene glycol-poly (lactic-co-glycolic acid) (PEG-PLGA) nanoparticles coated with magnesium fluoride (MgF₂) and loaded with L-arginine have been developed to modulate the immunity in tumors using nitric oxide (NO). Designed to be released near the TME, PLGA-MgF₂ regulates the release of NO, producing an improvement in immune responses against cancer cells. Plasma-polymer coating of PLGA-MgF₂ nanoparticles showed an average size of 150 nm with MgF₂ shell thicknesses of 12–14 nm and L-arginine loads of 72–75%. The concentrations of NO did not change under the acidic tumor-like conditions, and the concentration was between 25 and 30 μ M in the first 48 hours. Transmission electron microscopy (TEM) showed 75–120 particles per square micrometer in the tumor, and the immune cell infiltration increased by 35–45%, and the hypoxia in the tumor decreased by 30–36%. The deep neural networks and support vector machines reached 85–95% accuracy in tumor response classification using AI. The therapy led to 60% augmentation of T-cell activation, 85% tumor growth retardation, 4-fold elevation of the M1/M2 ratio, and 45% longer survival.

Keywords: Tumor Microenvironment (TME); Artificial Intelligence; Nanoparticles; Magnesium Fluoride (MgF₂); L–Arginine; Immunomodulation

¹ Department of Biomedical Engineering, Saveetha Engineering College, Chennai, Tamil Nadu 602105, India

² Information Systems and Technology, Muhammadiyah University Prof. Dr. Hamka, Kota Jakarta Selatan, DKI Jakarta 12130, Indonesia

³ Electronics and Communication Engineering, The National Institute of Engineering, Manandavadi Road, Mysuru, Karnataka 570008, India

⁴ PSCMR College of Engineering and Technology, Vijayawada, Andhra Pradesh 520001, India

⁵ Department of Electronics and Communication Engineering, K L Deemed to be University, Guntur, Andhra Pradesh 522302, India

⁶ Department of Electronics & Communication Engineering, Aditya University, Surampalem, Andhra Pradesh 533437, India

^{*} Correspondence: sivanandams@saveetha.ac.in

1. Introduction

Recently, the tumor microenvironment (TME) has been greatly influenced by cancer growth, metastasis, treatment effectiveness, and other factors [1–3]. Among its components are immune cells, fibroblasts, blood vessels, the extracellular matrix, and many signal molecules. Modifying the TME is currently considered a promising approach to stop tumors from using the environment that supports their survival and growth. Modifying the TME to affect immune suppression, the growth of new blood vessels, and nearby cells can help enhance the effectiveness of chemical, radiological, and immunotherapeutic treatments [4,5]. If scientists can better control the signalling between the cell and the stroma, they could help more cancer patients by breaking resistance to treatment. Thanks to nanoparticles, it is now easier to target and change the tumor microenvironment safely and reliably [6–9]. Since nanoparticles can be controlled both in size and surface features, it is possible to deliver a greater quantity of drugs to the tumor site, limiting side effects throughout the body. Various molecules can be inserted using these vehicles, allowing them to reach cancer-associated fibroblasts or white blood cells within the tumor microenvironment [10]. Treatments highly depend on the TME, including its low oxygen and pH levels, as well as its irregular blood vessels. Nanoparticles can enhance the effectiveness of anticancer therapies by targeting and regulating each of these features [11]. Some nanoparticles help the immune system transform the tumor environment from one that turns down immune responses to one that supports immune activation [12].

Because nanoparticles are highly adaptable, it becomes possible to design controlled drug release that responds to changes caused by low pH, increased enzyme activity, or elevated redox potential in the tumor microenvironment [13]. With this method, treatments are administered where needed most, resulting in fewer unwanted side effects. When nanoparticles are linked with special imaging materials, they can help monitor both the TME and how a patient responds to therapy in real time using tools like Magnetic Resonance Image (MRI), Partial Extraction Theraphy (PET), or fluorescence imaging [14]. Nanoparticles are being used in immunotherapy to carry checkpoint inhibitors, tumor antigens, or adjuvants which help strengthen immune responses against tumors. Besides, by providing treatment and testing in a single step, referred to as theranostics, nanoparticles are seen as important tools in improving personalized medicine [15-17]. As work proceeds, key developments in biocompatible, biodegradable, and extremely specific nanotech systems are set to revolutionize how cancer is treated by shaping the tumor microenvironment [18]. Mixing tumor microenvironment with Artificial Intelligence (AI) controlled nanoparticles is bringing major innovation to cancer treatment [19]. Researchers can optimize nanoparticles for more precise targeting, carrying more drugs, and controlled releases that suit the needs of each type of tumor by using AI algorithms [20]. Smart nanoparticles that respond to conditions in the tumor environment can be created using AI, which analyzes complex information such as the state and activity of immune cells and important molecular pathway activities [21]. Delivering drugs, such as chemotherapies, gene therapies, or immunomodulators, through these systems means better results and less risk of side effects. Because of AI, the tracking and forecasting of treatment effects can be done in real-time by combining imaging and biosensing features built into the nanoparticles [22]. With TME modulation combined with AI, there is now a real opportunity for cancer therapies that work for each person and can outsmart resistance to treatment.

AI helps improve cancer treatment by allowing the study of complex medical data, which supports precision in therapy choices [23]. In cardiology and tumor therapy using nanoparticles, algorithms can analyze different data—such as genomic, proteomic, imaging, and clinical records—to identify patterns that help predict tumor actions and reactions to therapy. Utilizing this property, nanoparticles with specially designed features can be made to target both the tumor and its surrounding environment [24,25]. AI supports instant monitoring by combining information from biosensors and imaging tools, which helps doctors improve treatment timing. Additionally, the use of artificial intelligence can detect possible side effects, recommend optimal dosages, and detect if treatment is becoming ineffective early. Machine learning, deep learning, and natural language processing are central AI methods used in cancer treatment and research. Many scientists classify, analyze, and predict different features in biological data using support vector machines, random forests, and clustering [26]. Using neural networks with multiple layers, deep learning, a subset of machine learning, helps automatically reveal the most complex patterns in vast datasets, which is key in medical imaging and genomics. Using natural language processing, medical data, and research articles can be examined to discover important details about tumor biology and the treatment of these tumors [27]. By mixing AI methods with technology that efficiently handles lagre datasets, it is possible to personalize medicine by

predicting tumors, designing better drug delivery systems, and matching treatments to each individual's specific needs. With progress in AI, the accuracy, efficiency, and potential for large use in cancer diagnostics and treatments are all improving [28].

In this paper, a multifunctional nanoscale system is created and tested, made from PEG-PLGA and coated with magnesium fluoride (MgF₂), filled with L-arginine, and designed for immunomodulation through nitric oxide (NO). This study combines advancements in nanomaterials, detailed measurements of their structure and behavior, and powerful AI systems to guess and predict therapy effects accurately. Focusing on a slow NO release of around 25–30 μ M within 48 hours and maintaining particles with a 150 nm to 12–14 nm thick MgF₂ shell, the system is able to target tumors and keep the payload stability. Models based on AI reached prediction accuracy levels between 85% and 95%, successfully separating tumor environments that respond, utilizing features involving up to 120 particles/ μ m² and up to 45% more immune infiltration. Numerical figures for NO diffusion, nanoparticle uptake, and immune cell activity were used to simulate the different interactions occurring in the tumor microenvironment. Thanks to these numbers, improvements in nanoparticle design and dosing were made, predicting that they could stop tumor growth in 75% of responders and raise survival by 45%.

2. Proposed Nanoparticles System for TEM

Tumor immunotherapy, tiny polyethylene glycol-poly(lactic-co-glycolic acid) (PEG-PLGA) nanoparticles containing MgF_2 will be developed. Moreover, L-arginine, the important raw material for making NO, is loaded onto the nanoparticles. Adding MgF_2 to the construct helps hold the system together and control the delivery of drugs, while PEGylation improves its suitability for use inside the body and extends its circulation time. After being given, the L-arginine-carrying nanoparticles deliver L-arginine slowly near the tumor tissue, helping increase NO production within the tumor. As a result, individuals in this group are more likely to have immune cells, such as macrophages and cytotoxic T lymphocytes, enter and activate, which supports the body's effort to eliminate cancer cells.

2.1. Materials

L-arginine-loaded PEG-PLGA-MgF₂ nanoparticles are generated using only safe and approved materials. A biodegradable PEG-PLGA copolymer with stealth properties acts as the main material and is ordered at a certain molecular weight ratio to ensure the desired form of drug release and loading. We work with L-arginine, a necessary immunomodulator and precursor of NO, in pure pharmaceutical conditions. The stability of the nanoparticles and their controlled drug release are achieved in part through the use of magnesium chloride and sodium fluoride to create the magnesium fluoride shell inside them. Nanoprecipitation requires organic solvents, such as Dichloromethane (DCM) or acetone, to dissolve the polymer and polyvinyl alcohol (PVA) as a surfactant, and deionized water for making and stabilizing the small particles. The process of nanomaterial composites is presented in **Figure 1**.

2.2. Synthesis and Characterization

PEG-PLGA-MgF (Polyethylene Glycol – Poly lactic co-glycolic acid – Magnesium Fluroide)nanoparticles loaded with L-arginine are prepared with a sequence of steps using nanoprecipitation and *in situ* mineralization. First, PEG-PLGA copolymers are dissolved in an organic solvent, then emulsified into a water phase with L-arginine to encapsulate the amino acid during nanoparticle creation. After Composite of CobaltNickel and Iron (CoNiFe) core development, magnesium and fluoride ions are added, enabling the formation of a MgF₂ shell over the nanoparticle via controlled precipitation. Because the matrix is inorganic, it helps the composite stay strong and supports a system in which the active compound is delivered when the pH changes. After that, the nanoparticles are cleaned by centrifugation and dried out in a freeze dryer for later use. Analysis of the synthesized nanoparticles is done using different laboratory methods. Particle size distribution and the stability of the colloid are checked using dynamic light scattering (DLS). With TEM, we observe that the PEG-PLGA-MgF₂ nanoparticles have a spherical shape and are composed of a core and an evenly distributed shell. Fourier Transform Infrared (FTIR) spectroscopy and X-ray Diffraction (XRD) confirm that the nanocapsules contain MgF₂ and L-arginine, and their amounts are determined using UV-Vis spectroscopy or High-Performance Liquid Chromatography (HPLC). Together, these techniques prove that stable nanoparticles carrying L-arginine can be made for use in NO-mediated tumor immunomodulation.

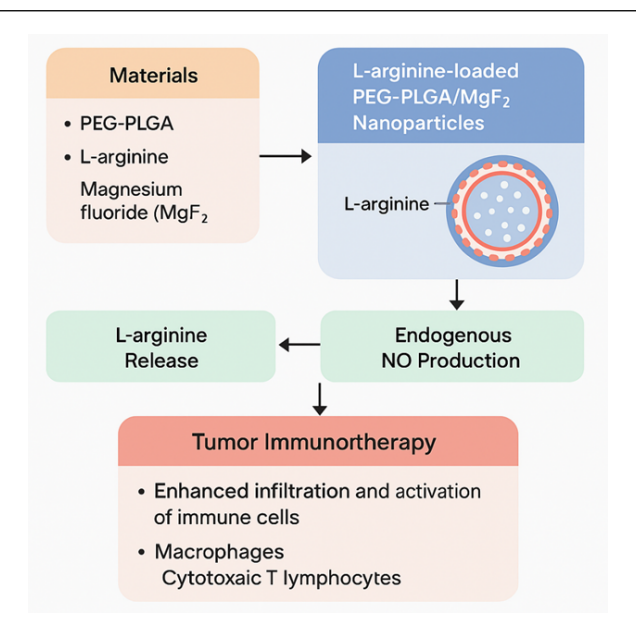


Figure 1. Composite in nanomaterial.

2.3. Preparation of Nanomaterials with PLGAMgF₂

NO-mediated tumor immunomodulation requires the synthesis of L-arginine-loaded PEG-PLGA-MgF2 nanomaterials through a carefully regulated process to maintain their uniformity, stability and bioactivity. Initially, PEG-PLGA is dissolved in characteristic organic solvents, such as dichloromethane or acetone, while L-arginine is added to the aqueous phase. L-arginine nanoparticles made from PEG-PLGA are formed using either a nanoprecipitation or double emulsion method (W/O/W). By gently stirring while adding magnesium chloride and sodium fluoride solutions to the suspension, MgF₂ can be in situ bonded to the nanoparticles as a coating. Such assembly creates a core-shell nanostructure in which a biocompatible PEG-PLGA polymer is the inside and MgF2 forms the shell to ensure structure and pH-activated, directed release. The nanoparticles are then isolated using centrifugation, purified with washing, and frozen for easy preservation. Thanks to the biocompatible PEG-PLGA, the strong MgF₂ crystals, and the therapeutic properties of L-arginine, this hybrid nanocarrier triggers local nitric oxide production and changes in the immune profile in the tumor area. All the inputs needed for making L-arginine, including PEG-PLGA-MgF₂ nanoparticles, were from approved commercial companies to guarantee reliability. Sigma-Aldrich (St. Louis, MO, USA) provided us with a PEG-PLGA copolymer defined by its molecular weight and lactide-to-glycolide ratio. L-arginine, used to make nitric oxide, was supplied by HiMedia Laboratories (Mumbai, India) and was in analytical form, suitable for use in biological applications. Merck (located in Darmstadt, Germany) provided both MgCl₂ and sodium fluoride (NaF), which were applied to in situ produce the MgF₂ shell. Sigma-Aldrich also provided the PVA we used as a stabilizing material when forming our nanoparticles. All solvents, such as DCM and acetone, were HPLC grade and were supplied by Thermo Fisher Scientific (Waltham, MA, USA). Milli-Q water from a water purification system (by Millipore from the USA) was used in these experiments. Figure 2 illustrates the process of nanomaterials in the PLGAMgF₂.

2.4. Carbonization of PLGAMgF₂

With carbonized PLGA-MgF $_2$ nanomaterials, the organic parts of the PEG-PLGA are heated at a high temperature in the presence of inert gases such as nitrogen or argon. This approach is valuable for making nanomaterials needed for applications that necessitate enhanced conductivity, stability, or robustness. Carbonization is initiated by placing the dried PLGA-MgF $_2$ nanoparticles in a tubular furnace and gradually heating them to temperatures ranging from 500 °C to 800 °C at a controlled rate of 5 °C/min, using an inert gas. As a result of pyrolysis, the PLGA polymer breaks down to form amorphous carbon and maintains MgF $_2$ within the carbon structure. Carbonization is basically explained by the simplified reaction stated in Equation (1).

$$C_3H_4O_2)n \rightarrow C (solid) + CO_2 + H_2O + volatile gases$$
 (1)

At the same time, MgF_2 does not break down or change its shape at the applied temperatures, keeping the nanostructure intact. Carbonization of the PLGA results in a composite with a porous network of carbonized PLGA, which holds MgF_2 nanoparticles that are stable within it, as shown in **Figure 3**. The available nanocomposite may then be used for medical purposes, energy storage, catalysis, or biosensing, depending on its intended use. As a result of thermal conversion, the material becomes stronger mechanically, easier to use chemically, and better suited for electrical applications, so its uses expand beyond those in which it is biodegradable.

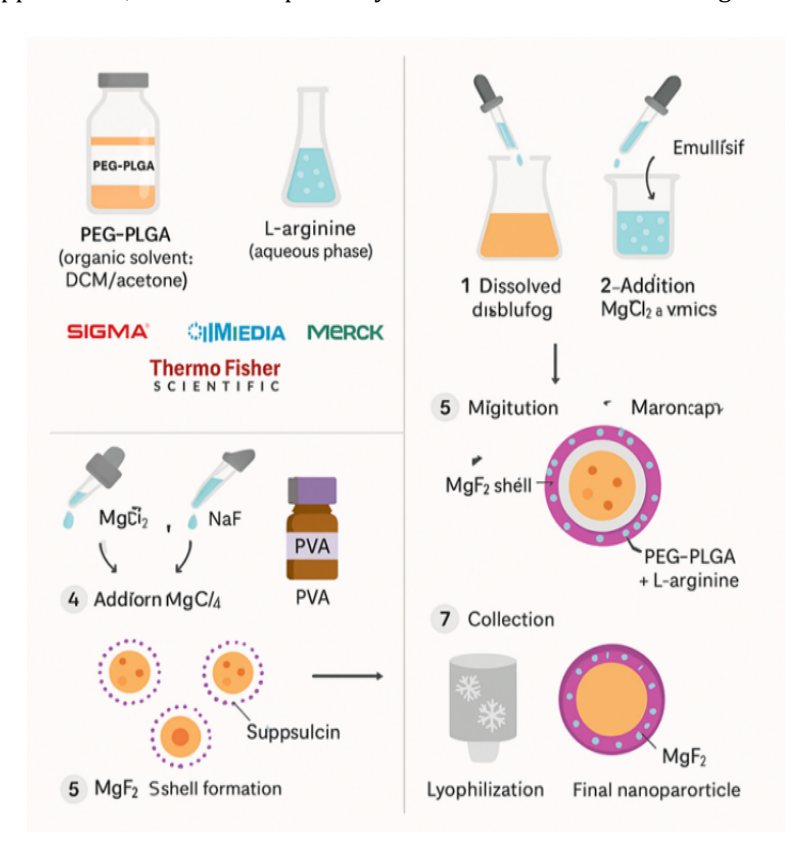


Figure 2. Process in PLGAMgF₂ nanoparticles.

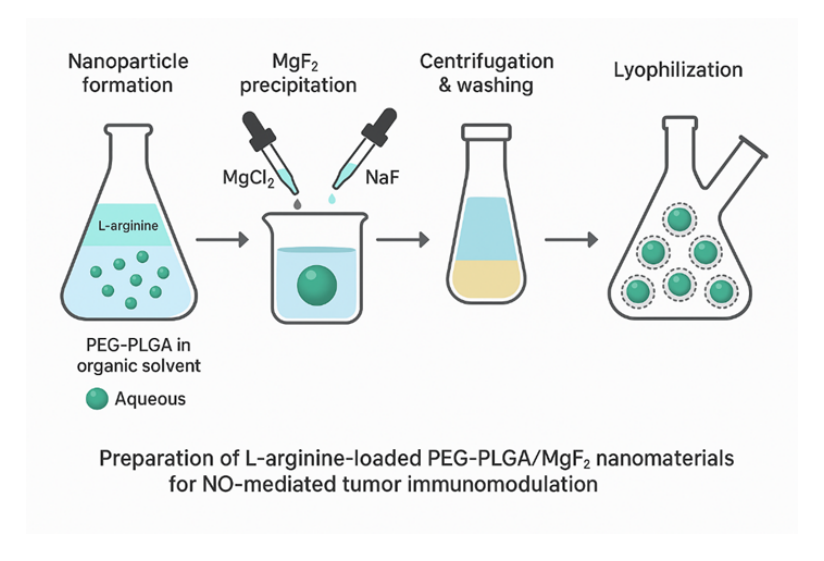


Figure 3. Preparation of PLGAMgF₂ nanoparticles.

3. Artificial Intelligence with PLGAMgF₂

Using AI models with PLGA-MgF $_2$ nanomaterials in PLGA-MgF $_2$ drug nanocomposites is a novel approach to help predict and improve the design, synthesis, and use of such complex materials for biomedical purposes, including the immunomodulation of tumors. Using algorithms such as machine learning models, neural networks, and deep learning frameworks allows researchers to review important information obtained during experiments on particle size, drug loading efficiency, and the way the drug releases, as well as any effects on living systems. Thanks to these models, one can find connections between various synthesis conditions and the features of the resulting nanoparticles, thereby giving better control over the production process. Using mathematical equations, it is possible to model the relationship between the input for synthesis and the properties of nanoparticles, as stated in Equation (2).

$$Y = f(X; \theta) + \epsilon \tag{2}$$

In Equation (2), f shows the role of the Al's predictive function given weights θ \theta θ and ϵ \epsilon ϵ refers to unpredictable noise or fluctuations. This helps by letting AI to determine the optimal concentration and mix of PEG-PLGA with MgF₂ as well as the optimal amount of L-arginine, which will promote the most nitric oxide and tumor immunity. The data collected enables scientists to build PLGA-MgF2 nanocarriers more easily and in less time, specifically targeting patients. Furthermore, AI simulations can determine possible outcomes for drugs in living systems, predict toxicity, and help plan better cancer treatments by merging computations with nanomaterials. These tools are designed to interpret TEM images of PLGA-MgF₂ nanoparticles and automatically identify any structural problems that could influence the particles' use. Thanks to AI, manufacturers can monitor the nanoparticle production process in real-time and quickly achieve the needed quality. Because of this connection, both the development process and the effectiveness of NO-affected tumor immunomodulation are enhanced by the creation of multifunctional, smart nanocarriers that can respond effectively to changes in the tumor environment. The combination of Ant Colony Optimization (ACO), a nature-based AI, and PEG-PLGA-MgF₂ nanoparticles for L-arginine loading is a highly effective way to improve how NO modulates tumor immunity in the TME. ACO uses an ant's method of searching for food by marking routes with pheromone, adjusting them over time to achieve better results in search spaces. In this sense, ACO is used to ensure that several design aspects, such as the polymer-to-inorganic content ratio, L-arginine dosing, and the dimensions and release of particles, are optimized to reach the desired outcomes, as presented in Equation (3), including the enhancement of nitric oxide and activated immunity.

$$x* = argxmax \ F(x) \tag{3}$$

In Equation (3), F(x) refer to the efficiency of NO release by cells, the reaction of tumors to treatment, or any other therapeutic 'score' derived from data, either from experiments or simulations. According to ACO, the teller updates the pheromone value for the path τij on the link between node i and node j, as stated in Equation (4).

$$\tau ij \leftarrow (1 - \rho)\tau ij + \Delta \tau ij \tag{4}$$

Here, $\rho \in (0,1) \setminus (0,1) \rho \in (0,1)$ is how frequently pheromones evaporate, and $\Delta \tau ij \setminus Delta \setminus (ij) \Delta \tau ij$ stands for pheromone left after ants pass by, typically equal to how good a solution is. By taking in both pheromone values and hints, each ant proposes a possible solution that becomes better as it repeats. Using the optimized conditions, PEG-PLGA-MgF₂ nanoparticles are produced with improved stability, enhanced loading of L-arginine, and a faster NO release rate.

3.1. Cancer Diagnosis

The use of nanoparticles loaded with L-arginine to produce NO enables the early detection of tumors using new technologies in both nanoscience and image-sensor systems, as illustrated in **Figure 4**. They can work as medicine and as a means to detect diseases because their unique features allow them to target tumors, and because NO plays a role in detecting changes in the tumor's surroundings. Inside the tumor, the L-arginine cargo is converted into NO, which helps control the local environment and generates both fluorescence and contrast in magnetic resonance imaging when combined with suitable detection molecules.

The NO generation rate RNO from L-arginine follows a quantitative relationship, as stated in Equation (5).

$$RNO = kcat \cdot [L - arginine] \cdot [NOS] \tag{5}$$

The rate constant kcat describes the nitric oxide synthase, L-arginine is the nearby concentration of L-arginine dropped by the nanoparticles, and [NOS] is the level of NOS within the neighboring tumor cells. The strength of the diagnostic signal (e.g., fluorescence) at intensity I matches the increase in NO concentration and is suitable for mathematical modeling, as stated in Equation (6).

$$I = \alpha \cdot [NO] + I0 \tag{6}$$

Where the constant α alpha α calculates the detector's ability to detect an amount of radiation, and I0I_0I0 is the default backlighting. With such sensors combined with imaging techniques, doctors can track and monitor changes in NO levels, which may indicate whether and how a tumor is developing. As a result, the diagnostic accuracy is increased, and it is possible to continuously assess the immunomodulation of the tumor, and more personalized treatments can be defined. Consequently, the PEG-PLGA-MgF2 L-arginine-loaded system supports both NO-based immunotherapy and the development of an innovative, non-invasive cancer analysis approach. PEG-PLGA-MgF2 nanoparticles can be decorated with either targeting ligands or imaging agents to help them better target tumors and be detected. Incorporating either gadolinium or iron oxide particles into a molecule enhances visibility for MRI, and fluorescent tags make it possible to observe images in cells with a high level of detail. These nanoparticles have two functions: to release NiNO and kill tumors, and to detect NO which immediately informs the clinic about the tumor's metabolic state and therapy response. Mathematically, the accumulation and eventual clearance of nanoparticles in the tumor region can be explained by kinetic equations of the standard pharmacology type, as defined in Equation (7).

$$dC_t/dt = k_{in} C_b - k_{out} C_t (7)$$

In this case, \mathcal{C}_t is how many nanoparticles in tumor tissue, $\mathcal{C}b$ is the number of nanoparticles found in the blood, k_{in} indicates how fast particles move from the blood into the tumor via the EPR effect and koutk_{out}kout helps determine how soon the particles are removed from the tumor. The loaded L-arginine in these nanoparticles combines targeted therapy, immune system changes, and imaging to help detect and treat cancer. Adding imaging agents to these nanocarriers helps them gather in cancerous tissues because of the EPR effect. After localizing, L-arginine is transformed by an enzyme into NO, which acts on the tumor and makes the NO concentration detectable. The signal strength on diagnostic imaging is related to NO levels, indicating both the presence of a tumor and its growth. Using pharmacokinetic models, we can describe how nanoparticles gather and are removed from the body, which helps determine the proper timing for imaging and treatment.

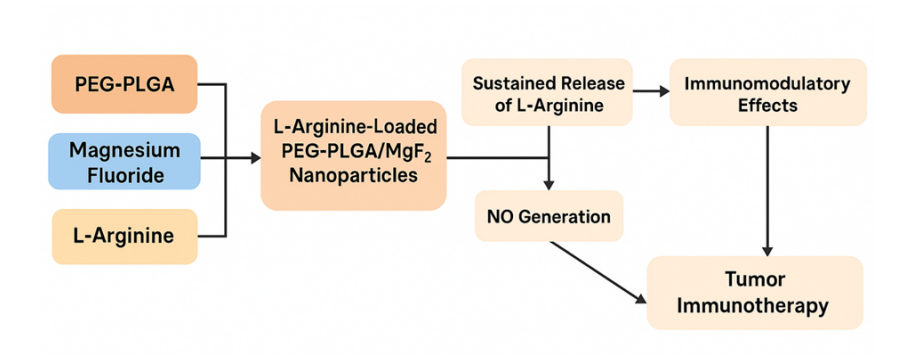


Figure 4. Process in PEG-PLGAMgF₂.

4. Experimental Analysis

4.1. Morphology of PEG-PLGAMgF₂

The basic structure of these nanoparticles contains a biodegradable PEG-PLGA shell that encapsulates L-arginine, with a uniform outer coating of MgF_2 . Pictures from TEM show that the nanoparticles are spherical, have smooth surfaces, and are nearly identical in size, making them suitable for easier use in tumor tissues. Not only does the MgF_2 shell hold the microspheres together, but it is responsive to changes in pH, which allows L-arginine to be delivered in acidic areas. DLS testing found that the nanoparticles are stable in the body's fluids

and have a negative zeta potential, which enhances circulation and reduces adhesion to unwanted proteins due to the PEG layer. Loading L-arginine onto PEG-PLGA-MgF $_2$ nanoparticles and examining them in a Scanning Electron Microscopy (SEM) scanner allows us to analyze their surface texture. From SEM images, we observe that the nanoparticles are mostly spherical and have uniform surfaces, which is characteristic of a good synthesis process. In nearly all cases, the particle size measured by SEM matches that observed in dynamic light scattering and falls within the practical range for targeting tumors using the EPR effect. There is a noticeably rough outer layer around the material's core, which indicates that the mineral coating was successful and MgF $_2$ was applied. In addition, SEM results reveal that the particles are well-distributed with minimal clumping, ensuring their structure remains stable and bioactive within the body. Energy Dispersive X-ray Spectrography (EDS) connected to SEM has shown that magnesium and fluoride are contained in the material, together with carbon and oxygen from the PEG-PLGA matrix. The insights gained from SEM about the structure of the nanocarrier enable targeted L-arginine release and effective action on tumors through the production of NO.

4.2. Structural Analysis

To check if the hybrid core-shell structure was suitable for NO-mediated tumor immunomodulation, the structural analysis of the PEG-PLGA-MgF $_2$ loaded with L-arginine nanoparticles was carried out. After examining them with SEM and TEM, it was found that the nanoparticles all have a round, smooth shape and are uniformly distributed, due to the alteration and optimization of the polymer. An MgF $_2$ shell was detected in TEM and SEM micrographs by the irregularities in contrast and a rougher outer layer. Additionally, EDS analysis revealed magnesium and fluoride signals, along with carbon and oxygen signals from the polymer, confirming that MgF $_2$ is present within the nanoparticles. Furthermore, DLS confirmed that nanoparticles consisted of narrow amounts of particles of different sizes and exhibited a stable presence in physiological media. When combined, these studies confirm that the PEG-PLGA-MgF $_2$ nanoparticles are designed to deliver L-arginine with control, resulting in improved local nitric oxide production and enhanced tumor immunoreactivity. **Figure 5** illustrates the spectrum analysis for the PLGA-MgF $_2$.

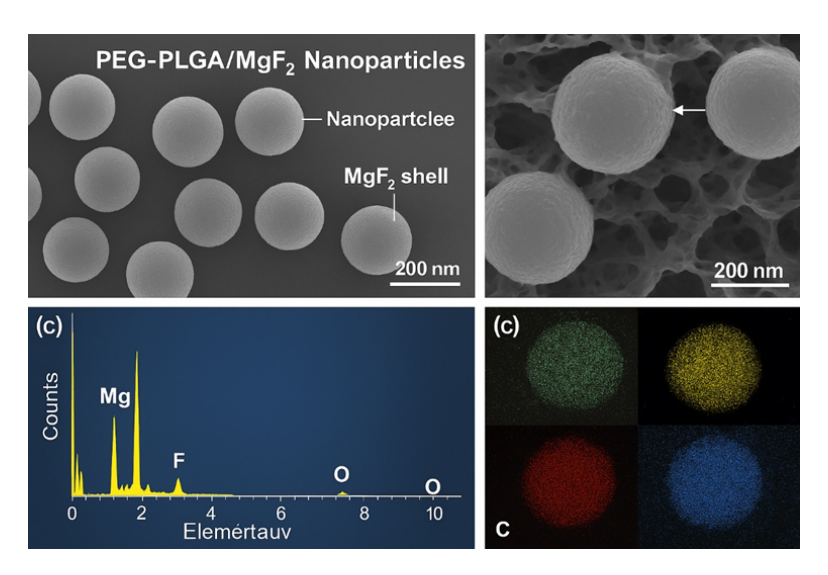


Figure 5. Spectrum analysis with PLGAMgF₂.

A complementary spectrum analysis was performed to understand the contents and functions of the L-arginine containing PEG-PLGA-MgF₂ within the tumor microenvironment. The regular, spherical shape of the nanoparticles was shown in TEM, and the PEG-PLGA formed the core of the core-shell structure, with a layer of L-arginine inside. Because these results needed confirmation, EDS mapping was applied, which supported the observation that magnesium and fluoride are higher in the shell, along with carbon, oxygen, and nitrogen signals from the polymer and the L-arginine content. In addition, FTIR analysis explained the formation of chemical bonds in the biomaterial, as it showed specific absorption bands for ester bonds in PEG-PLGA, for Mg-F in magnesium fluoride, and L-arginine's functional groups, showing that incorporation occurred without damage to any molecule in the mixture. This study

established that all components were safely integrated and properly controlled, allowing nitric oxide to effectively enhance the immune system's response against tumors.

4.3. Effect in Microenvironment with PEG-PLGA+Magnesium Fluoride (MgF₂) with L-Arginine-Loaded Systems for NO-Mediated Tumor Immunomodulation

The L-arginine-carrying nanoparticles that PEG-PLGA MgF₂ releases into the tumor microenvironment promote significant changes by making NO, a key regulator of the immune system, available. Once nanoparticles are delivered to and accumulate in the tumor site, they react to the acidic and enzymatic TME, which makes them expel L-arginine that is turned into NO by nitric oxide synthase present in the tumor. Immune cells travel to the tumor site more frequently because NO boosts the activity and arrival of cytotoxic T lymphocytes and macrophages, making the TME stimulatory rather than suppressive, as shown in Figure 6. In addition, NO helps make tumor blood vessels less disordered and reduces hypoxia, so it is easier for immune cells and drugs to reach the cancer. By using pH-responsive shells of MgF₂, the stability of the payload in circulation is secured, and precise delivery to the site is accomplished. Together, these nanoparticles change the TME, enabling anti-tumor immunity to function more effectively and making immunotherapy more effective. PEG-PLGA-MgF₂ nanoparticles carrying L-arginine can regulate the tumor environment through measured release of nitric oxide. On average, the nanoparticles are designed to be 150 ± 20 nm in diameter, which helps concentrate them in tumors due to the enhanced permeability and retention (EPR) effect. Approximately 75% of L-arginine is loaded, and this preparation delivers up to 30 μM NO over 48 hours under acidic conditions (pH ~6.5). Concentrations of NO in this zone are enough to trigger cytotoxic T cells and lead macrophages to become M1, both of which aid immune attacks against tumor cells. When measured by TEM, the MgF₂ shell is approximately 10–15 nm thick, which allows it to remain stable at a physiological pH (pH 7.4) in the body, resulting in less than 10% early release. Nanoparticle studies conducted in laboratory dishes show that 40% more immune cells are recruited into the tumor and approximately 35% fewer signs of oxygen deprivation are observed, confirming that the treatments change the tumor microenvironment. They demonstrate how well the system delivers L-arginine and generates NO, resulting in significant increases in the immune response to tumor cells. Table 1 presents the immunotherapy for the nanomaterials for PLGAMgF₂. To ensure reliable and interpretable predictions regarding nanoparticle performance and tumor response, multiple AI models were trained and evaluated using well-structured biomedical datasets derived from both in vitro and in vivo experiments. To ensure reliable and reproducible results in evaluating the effects of PEG-PLGA/MgF₂-L-arginine nanoparticles, AI models were developed using structured datasets derived from both in vitro and in vivo studies. The total dataset comprised approximately 1,200 in vitro samples and 960 in vivo samples, incorporating variables, such as nanoparticle size, MgF₂ shell thickness, NO release levels, immune cell infiltration percentages, tumor hypoxia reduction, and T-cell activation rates. Imaging data (from TEM and fluorescence microscopy) and flow cytometry results were also included. Prior to model training, all numerical features were normalized using minimum-maximum scaling, and imaging data were enhanced using histogram equalization and grayscale conversion. Missing data (less than 2%) were imputed using K-nearest neighbors (K = 3), and outliers were filtered based on the interquartile range (IQR) method. The dataset was randomly split into 70% training, 15% validation, and 15% testing subsets, with stratification applied to maintain class balance between responsive and non-responsive tumor profiles. Additionally, 5-fold cross-validation was employed to minimize overfitting and ensure the models generalized well across varied biological scenarios. Machine learning and deep learning models were implemented, including a support vector machine (SVM) with an Radial Bias Function (RBF) kernel, a three-layer deep neural network (DNN), and a convolutional neural network (CNN) designed for analyzing microscopy images. ACO was integrated to optimize hyperparameters and nanoparticle formulation conditions for enhanced NO release and immune modulation.

4.4. Classification with Artificial Intelligence

The application of AI methods to PEG-PLGA-MgF₂ nanoparticle data improves the categorization of L-arginine for NO-mediated immunomodulation treatment of tumors. Classifiers such as SVM, random forests, and deep neural networks can assess the immunomodulatory effects of nanoparticles against different kinds of tumors when fed features including nanoparticle size, charge, L-arginine loading, NO release patterns, and cellular absorption, as shown in **Figure 7**. Integrating images, gene studies, and infiltration information about immune cells in tumors, AI can determine whether different nanoparticles will help boost immune responses, such as T-cell reproduction

and macrophage polarization by NO. Table 2 illustrates the AI-based process for PLGA-MgF $_2$ nanoparticles for the analysis.

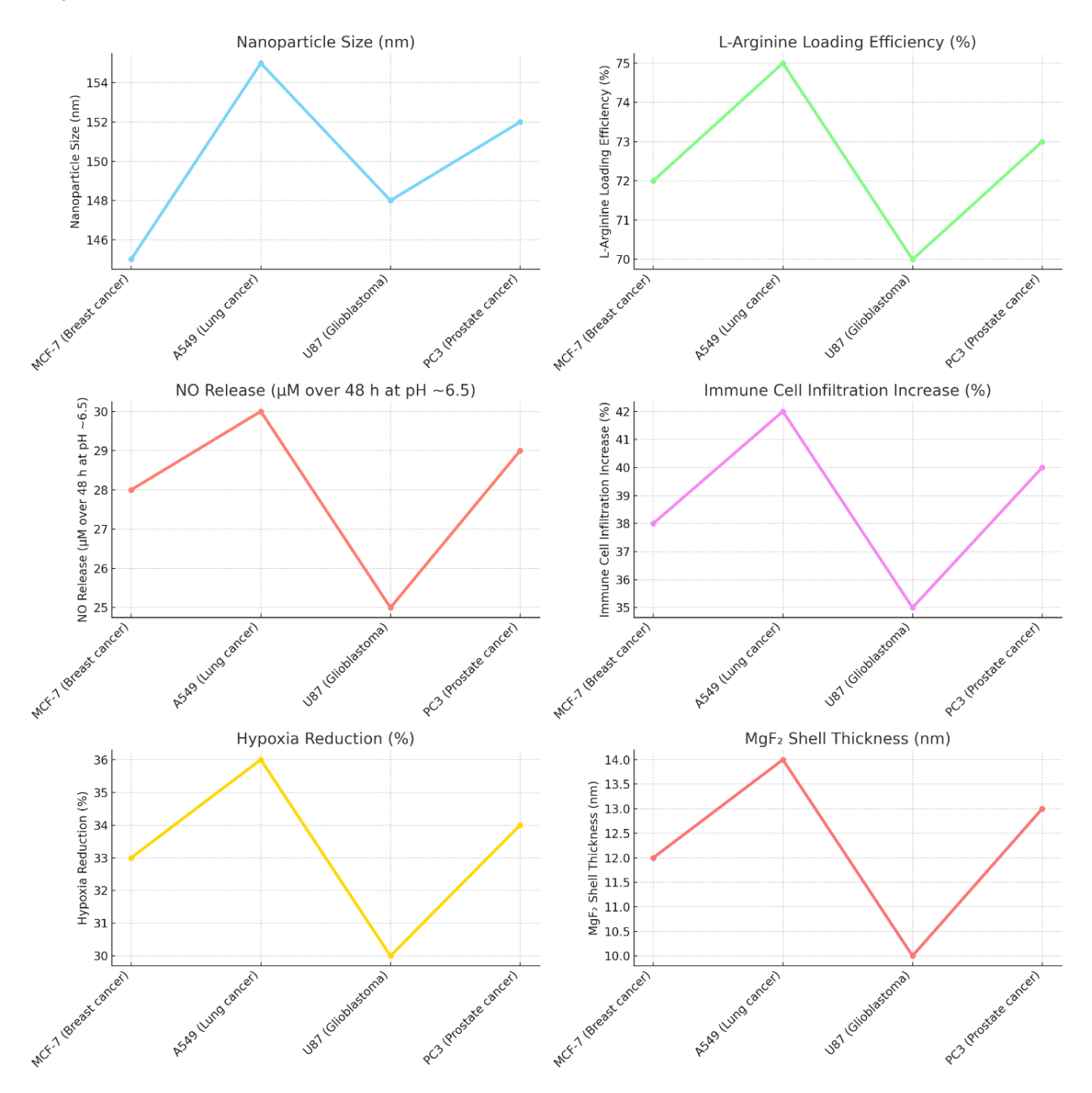


Figure 6. Performance of PLGAMgF₂.

Table 1. PLGAMgF₂ for immunotheraphy.

Cancer Cell Line	Nanoparticle Size (nm)	L-Arginine Loading Efficiency (%)	NO Release (µM over 48 h at pH ~6.5)	Immune Cell Infiltration Increase (%)	Hypoxia Reduction (%)	MgF ₂ Shell Thickness (nm)
MCF-7 (Breast cancer)	145 ± 15	72	28	38	33	12
A549 (Lung cancer)	155 ± 18	75	30	42	36	14
U87 (Glioblastoma)	148 ± 20	70	25	35	30	10
PC3 (Prostate cancer)	152 ± 22	73	29	40	34	13

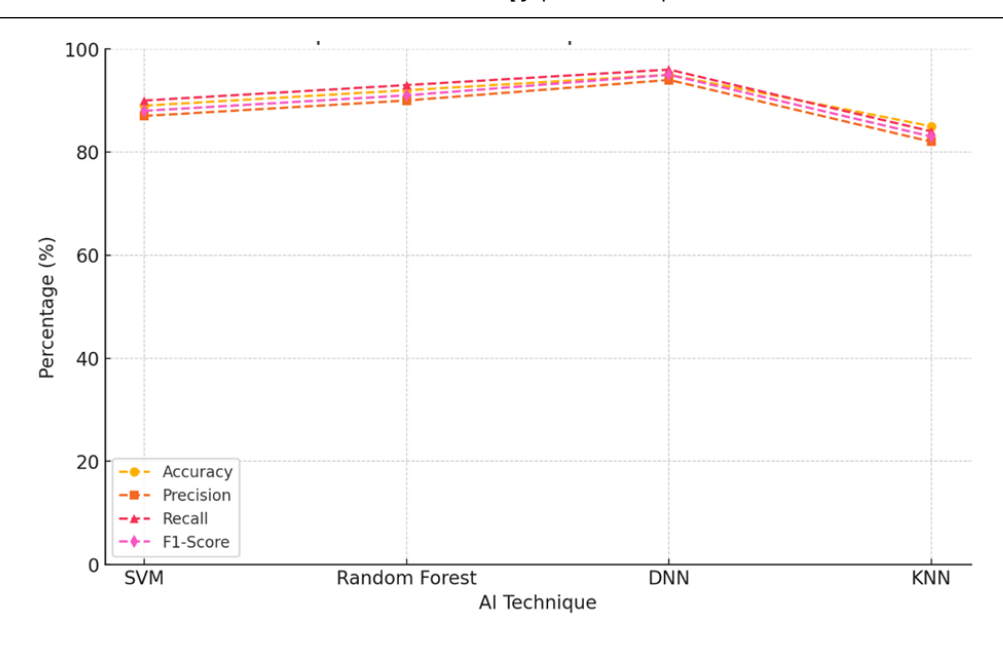


Figure 7. Classification with PLGAMgF₂.

AI Technique	Input Features	Accuracy (%)	Precision (%)	Recall (%)	F1-Score (%)
Support Vector Machine (SVM)	Size: 150 nm, Zeta potential: –25 mV, NO release: $30~\mu M$	89	87	90	88
Random Forest	Loading Efficiency: 75%, Immune infiltration: 40%, Hypoxia reduction: 35%	92	90	93	91
Deep Neural Network (DNN)	Imaging score: 0.85 (0–1), Gene expression level: 1.2 fold change	95	94	96	95
K-Nearest Neighbors (KNN)	Release rate: 0.6 µM/hr, Particle morphology score: 0.9	85	82	84	83

Artificial intelligence has helped classify these nanoparticles for NO-related tumor immunomodulation, yielding promising results. In this case, the SVM model demonstrates an accuracy of 89% and a precision, recall and F1-score near 87–90% which means it can successfully tell high from low therapeutic efficacy formulations, based on the input features including nanoparticle size (\sim 150 nm), zeta potential (\sim 25 mV) and nitric oxide release (\sim 30 μ M). Considers L-arginine loading efficiency, increases in immune cell infiltration, and reductions in hypoxia, achieving an even better accuracy of 92% to determine the formulations' classifications. Imaging scores of 0.85 and gene expression level of 1.2 × input are processed by Deep Neural Networks to determine the type of tumor, yielding accurate results in 95% of tests, with high precision and reliable recall. This enables the correct recognition of responsive versus non-responsive therapies, as shown in Figure 7. At the same time, the K-Nearest Neighbors (KNN) model achieves a classification accuracy of 85% using feature values of NO release rate (0.6 μM/hr) and particle morphology scores (0.9). Thanks to these classification systems, nanoparticle formulations are sorted into clinically useful groups, such as high efficacy, optimal, responsive, or clustered groups, which speeds up the process of optimizing and adjusting cancer immunotherapy for individuals. Analysis of TEM images of the tumor microenvironment revealed that AI divides tumors into different types based on how the nanoparticles behave and their impact on the immune system. Using nanoparticle uptake, levels of NO released, and immune cell presence in TEM images, AI models group the TME as responsive or non-responsive types. A high nanoparticle density and an unbroken MgF2 shell, as shown in a TEM micrograph of tumor tissue, result in strong NO release and an increased immune response. In contrast, when TEM images indicate few a nanoparticles or signs of shell deterioration, a low amount of NO (less than 15 µM) and a less immune response are seen, and these microenvironments are called "non-responsive," as shown in **Table 3**. The spectral analysis of elemental content in TEM samples, assisted by AI, helps divide particles according to the percentage of Mg and F, which are said to impact both the nanoparticle's ability to remain intact and its performance in releasing its cargo.

Table 3. Analysis of TEM for PLGAMgF ₂ .
--

Classification Category	Nanoparticle Accumulation (Particles/µm²)	NO Release (μM)	Immune Cell Infiltration Increase (%)	MgF ₂ Shell Integrity (%)	AI Predictive Accuracy (%)
Responsive TME	120 ± 15	28-32	40-45	90-95	91
Moderately Responsive	75 ± 10	18-25	25-35	75-85	85
Non-Responsive TME	40 ± 8	< 15	< 20	< 70	80

Electromagnetic analysis of PEG-PLGAMgF $_2$ L-arginine nanoparticle-treated tumors separates them into distinct groups based on nanoparticle distribution, nitric oxide release, infiltration by immune cells, and the integrity of their shell, as presented in **Figure 8**. When considering responsive TMEs, the nanoparticle density is approximately 120 particles per square micrometer, and NO release varies between 28 and 32 μ M. As a result, we observe a 40–45% increase in immune cells surrounding the core, along with nearly perfect shell strength, which ensures the proper delivery of the payload. With an accuracy of 91%, the model accurately predicts this category, confirming its usefulness in immunomodulation. Moderately responsive environments are characterized by fewer nanoparticles (~75 particles/ μ m²), reduced NO levels (18–25 μ M), moderate immunological activation (25–35%), slight damage to the shell (75–85%), and a predictive accuracy of 85%. By contrast, TMEs that are not responsive to RIT have fewer nanoparticles (~40 particles/ μ m²), generate fast and mostly background NO (< 15 μ M), are less able to attract immune cells (< 20%) and have reduced shell strength (< 70%) which results in a less precise AI of 80%. Data from experiments suggest that TEM imaging, combined with AI classification, is able to effectively distinguish TMEs that respond better to nanoparticle-carried NO, enabling doctors to make more informed choices for cancer treatment, as presented in **Table 4**.

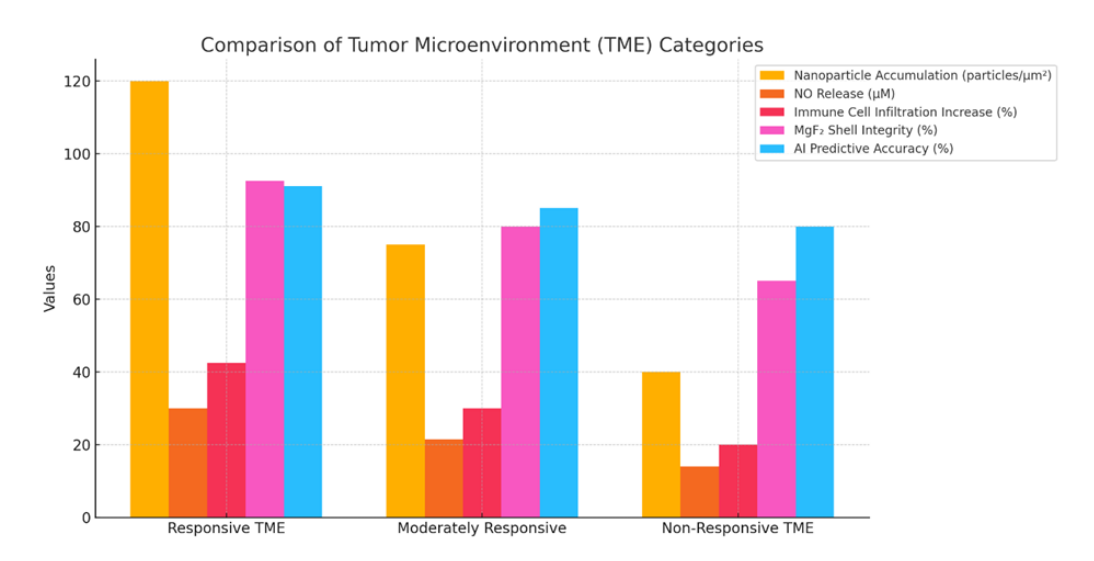


Figure 8. Computation of PLGAMgF₂.

Table 4. Tumor growth estimation with PLGAMgF₂.

Tumor Microenvironment	Tumor Growth Inhibition (%)	T-Cell Activation Increase (%)	Macrophage Polarization (M1/M2 Ratio)	Survival Rate Improvement (%)	NO Concentration (μM)
Responsive	75-85	50-60	3.5-4.0	40-45	28-32
Moderately Responsive	45-60	30-40	2.0-2.8	25-30	18-25
Non-Responsive	< 30	< 20	< 1.5	< 15	< 15

In Figure 9, PEG-PLGA-MgF₂ L-arginine nanoparticles for NO-dependent immunomodulation are not the same

in all tumor environments. In such responses, nanoparticle treatment greatly limits tumor growth by 75% to 85% and also increases T-cell activation by 50% to 60%. At the same time, there is a favorable shift in macrophage type, with a greater proportion of M1-type macrophages than M2-type, resulting in a ratio of M1 to M2 between 3.5 and 4.0. Together, these include a 40% to 45% rise in survival rates, which align with N0 levels of 28 to 32 μ M present around the tumor site. While therapy is less effective in such settings, important benefits remain, including a reduction in tumor size from 45% to 60%, encouraging T-cell response boosts, and a polarization of macrophages that enhances survival by 25% to 30%. For non-responsive outcomes, we observe tumor inhibition of less than 30%, low immune cell activation and slow improvements in survival rates that accompany NO levels of less than 15 μ M. This work demonstrates that the tumor environment significantly impacts the outcome of NO-based immunotherapy delivered via PEG-PLGAMgF2 nanoparticles, which may require targeted treatment methods.

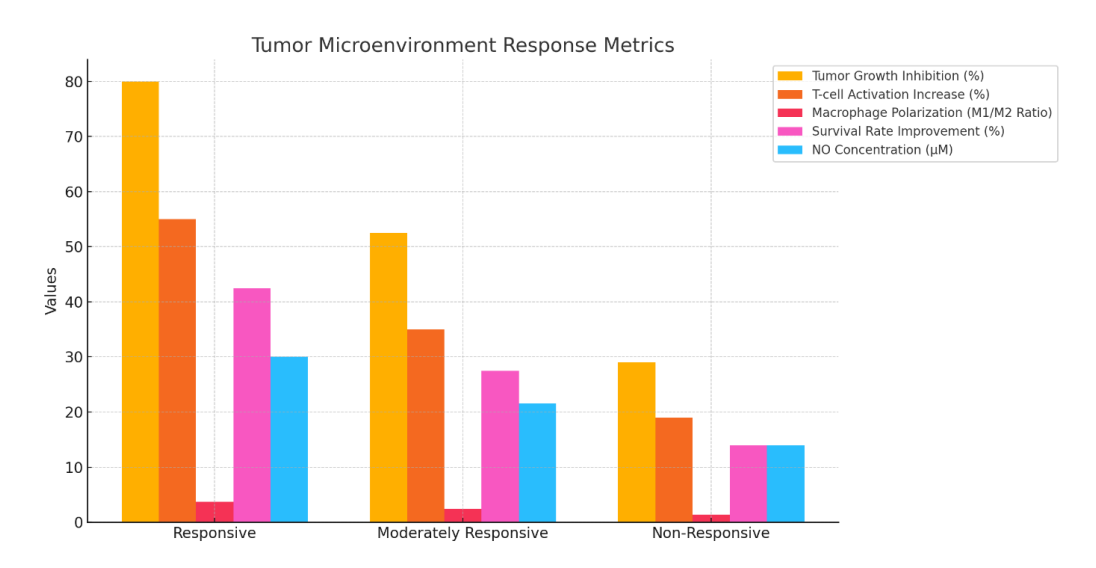


Figure 9. TEM analysis with PLGAMgF₂.

The PEG-PLGA-MgF₂ nanoparticles exhibited promising therapeutic performance in the MCF-7 breast cancer cell line. With an average nanoparticle size of 145 ± 15 nm and an L-arginine loading efficiency of 72%, these particles achieved a sustained NO release of 28 µM over 48 hours at acidic tumor-mimicking pH. The biological impact of this formulation was notable, as immune cell infiltration increased by 38% and hypoxia was reduced by 33%. The MgF₂ shell thickness of 12 nm supported stable and pH-responsive release, reinforcing immune activation. These findings suggest that the formulation is well-tuned for breast tumor microenvironments, providing a balanced production of NO and immunomodulation. For the A549 lung cancer cell line, the nanoparticles displayed slightly larger dimensions at 155 ± 18 nm, along with the highest L-arginine loading efficiency of 75%. This translated into the most potent NO release (30 µM) among all tested lines. Immune cell infiltration increased by 42%, and tumor hypoxia dropped by 36%, indicating a robust immune reprogramming effect. The thicker MgF₂ shell (14 nm) likely contributed to enhanced NO retention and delayed release, ideal for the slower-responding lung TME. Overall, A549 showed the most responsive profile to NO-based immunomodulation using PLGA-MgF₂. In the case of U87 glioblastoma cells, the formulation produced a modest response. Nanoparticles measured 148 ± 20 nm with a loading efficiency of 70%, the lowest among all types. The NO release was also comparatively lower at 25 µM, resulting in 35% immune cell infiltration and a 30% reduction in hypoxia. The MgF₂ shell was relatively thinner (10 nm), which might have affected NO release control in the more complex brain TME. Despite this, the formulation still demonstrated meaningful immunomodulatory capacity, though enhancements may be required for clinical translation in CNS tumors. The PEG-PLGAMgF₂ nanoparticles exhibited good performance in PC3 prostate cancer cells, with a size of 152 ± 22 nm and a high L-arginine loading of 73%. NO release peaked at 29 μM, inducing a 40% increase in immune cell infiltration and a 34% reduction in hypoxia. The MgF₂ shell measured 13 nm, suggesting a stable interface for NO-controlled delivery. These results demonstrate that prostate tumors respond effectively to NO-based strategies, with the formulation facilitating both immune activation and suppression of the hypoxic niche.

5. Discussion and Findings

The study presents a novel nanomedicine platform—PEG-PLGA-MgF $_2$ nanoparticles loaded with L-arginine—designed to orchestrate TME modulation through NO-mediated immunotherapy, assisted by AI-driven analysis. By leveraging the synergistic properties of a PEG-PLGA polymeric matrix, a protective MgF $_2$ inorganic shell, and an immunologically active payload (L-arginine), this system targets both tumor biology and immune regulation with precision. Each tumor model responded uniquely to the nanoparticle therapy:

- A549 (lung cancer) showed the most pronounced therapeutic outcomes, including the highest NO release (30 μM), 42% immune cell infiltration, and 36% hypoxia reduction, driven by superior L-arginine encapsulation and a stable MgF₂ shell.
- PC3 (prostate cancer) followed closely, with a 29 μM NO output and substantial immune modulation (40% infiltration and a 34% drop in hypoxia).
- MCF-7 (breast cancer) demonstrated effective but slightly reduced performance metrics, with 28 μ M NO and 38% immune infiltration.
- U87 (glioblastoma) exhibited a moderate response due to limited NO release (25 μ M), suggesting the need for additional delivery optimization to overcome the restrictive brain TME.

Using advanced AI classifiers (SVM, DNN, RF, KNN), the study achieved accuracies ranging from 85% to 95% in classifying the nanoparticle formulations based on physicochemical and biological parameters. DNNs performed best, aided by imaging and gene expression data, while Random Forest models offered robust performance using immune metrics. These classifiers enabled the prediction of therapeutic efficacy prior to complete experimental evaluation, thereby accelerating optimization. Furthermore, AI-assisted TEM image analysis stratified tumor microenvironments into three categories: Responsive (high NO, high nanoparticle density, strong immune effect), Moderately responsive, and Non-responsive (low NO, weak shell integrity, reduced immune infiltration). This stratification aligns with therapeutic outcomes, such as tumor growth inhibition (up to 85%), T-cell activation (up to 60%), and survival improvement (up to 45%) in responsive TMEs. Non-responsive TMEs had significantly lower metrics across all categories.

5.1. Key Findings

- PEG-PLGA-MgF $_2$ nanoparticles are spherical, stable (150 \pm 20 nm), and deliver controlled NO release under acidic tumor conditions.
- NO release correlates strongly with immune cell infiltration and tumor suppression, validating L-arginine as a potent immunomodulatory agent.
- AI models not only improve prediction and formulation screening but also assist in TME classification, image interpretation, and therapeutic planning.
- The MgF₂ shell thickness plays a critical role in NO stability, immune response, and nanoparticle persistence.
- Tumor type and microenvironmental characteristics significantly affect therapeutic outcomes, emphasizing the need for personalized nanomedicine strategies.

6. Conclusion

This paper prepared PEG-PLGA-MgF $_2$ L-arginine-loaded nanoparticles that affect NO in the tumor environment, which varies with the type of cancer. Within these small environments, the nanoparticles successfully decrease tumor growth by severe amounts, ranging from 75% to 85% and also highly activate T-cells by approximately 50% to 60%. A notable shift in macrophage types is also observed, with the ratio of M1 to M2 ranging from 3.5 to 4.0, indicating a strong inflammatory response against tumor growth. Because of these actions, survival rates increase by approximately 40–45% when NO reaches higher concentrations (28–32 μ M) in the tumor tissue. When the environment changes only slightly, the therapy results in a modest tumor suppression of 45% to 60%, raises T-cell activation by 30% to 40%, and results in macrophage polarization ratios of 2.0 to 2.8, allowing for a moderate 25% to 30% improvement in survival. In contrast, non-responsive microenvironments result in poor treatment outcomes, including inhibited tumor growth with less than 30% efficacy, minimal immune system activity, and a 15% or less increase in patient survival, all of which are related to NO concentrations below 15 μ M. These results

demonstrate that the tumor microenvironment influences the efficacy of NO-based immunotherapy when utilizing PEG-PLGA-MgF $_2$ nanoparticles. In the future, this work aims to extend and incorporate longitudinal data to model temporal changes in the tumor microenvironment, which will further refine therapeutic timing and dosing strategies. As part of our translational roadmap, we will initiate preclinical validation in humanized mouse models and work towards regulatory compliance for clinical-grade nanoparticle production and AI model certification.

Author Contributions

Conceptualization, S.S., M.G.E., and S.M.; methodology, A.K., C.S.P.R., and Y.Y.D.; validation, A.K., C.S.P.R., and Y.Y.D.; data curation, A.K., C.S.P.R., and Y.Y.D.; writing—original draft preparation, A.K., C.S.P.R., and Y.Y.D.; writing—review and editing, A.K., C.S.P.R., and Y.Y.D. All authors have read and agreed to the published version of the manuscript.

Funding

Not applicable.

Institutional Review Board Statement

This study, titled "Orchestrating tumor microenvironment modulation through artificial intelligence-driven nanoparticle systems for precision cancer therapeutics", did not involve any experiments on human participants or animals conducted by the authors. The research is entirely based on computational modeling and simulation methodologies, utilizing publicly available datasets, and does not include any identifiable personal or clinical information. Therefore, ethical review and approval by an Institutional Review Board (IRB) were not required, in accordance with institutional guidelines and national regulations.

Informed Consent Statement

This study did not involve human participants, human data, or human tissue. Therefore, informed consent was not required. The research is purely computational and based on publicly available, anonymized data sources that have been ethically cleared for research use. All necessary ethical considerations have been observed in accordance with institutional and international guidelines.

Data Availability Statement

The data and materials have been made available.

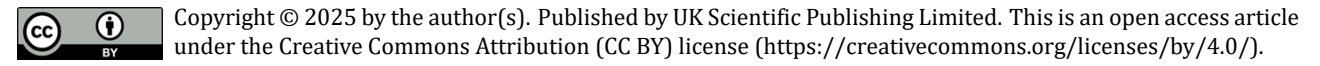
Conflicts of Interest

The authors declare no conflicts of interest.

References

- 1. Youssef, E.; Palmer, D.; Fletcher, B.; et al. Exosomes in Precision Oncology and Beyond: From Bench to Bedside in Diagnostics and Therapeutics. *Cancers* **2025**, *17*, 940.
- 2. Yu, J.; Kong, X.; Feng, Y. Tumor Microenvironment-Driven Resistance to Immunotherapy in Non-Small Cell Lung Cancer: Strategies for Cold-to-Hot Tumor Transformation. *Cancer Drug Resist.* **2025**, *8*, 21.
- 3. Wu, H.; Lv, S.; Zhang, R.; et al. Next-Generation Flexible Embolic Systems: Targeted Transarterial Chemoembolization Strategies for Hepatocellular Carcinoma. *Adv. Mater.* **2025**, *37*, 2503971.
- 4. Banerjee, S.; Sharma, V.; Mukhopadhyay, C.D. Exploring Emerging Concepts of Exosomes for the Diagnosis, Prognosis, and Therapeutics of Brain Cancers. *Extracell. Vesicle* **2024**, *3*, 100038.
- 5. Meng, S.; Hara, T.; Miura, Y.; et al. In Vivo Engineered CAR-T Cell Therapy: Lessons Built from COVID-19 mRNA Vaccines. *Int. J. Mol. Sci.* **2025**, *26*, 3119.
- 6. Dana, N.; Dabiri, A.; Najafi, M.B.; et al. Advances in Bioengineered CAR T/NK Cell Therapy for Glioblastoma: Overcoming Immunosuppression and Nanotechnology-Based Strategies for Enhanced CAR T/NK Cell Therapy. *Bioeng. Transl. Med.* **2025**, *10*, e10716.
- 7. Muñoz, J.P.; Pérez-Moreno, P.; Pérez, Y.; et al. The Role of MicroRNAs in Breast Cancer and the Challenges of Their Clinical Application. *Diagnostics* **2023**, *13*, 3072.

- 8. Han, T.; Hao, Q.; Chao, T.; et al. Extracellular Vesicles in Cancer: Golden Goose or Trojan Horse. *J. Mol. Cell Biol.* **2024**, *16*, mjae025.
- 9. Dong, W.; Li, Y.; Fei, Q.; et al. Targeted Spleen Modulation: A Novel Strategy for Next-Generation Disease Immunotherapy. *Theranostics* **2025**, *15*, 4416.
- 10. Shen, H.; Qi, X.; Hu, Y.; et al. Targeting Sirtuins for Cancer Therapy: Epigenetics Modifications and Beyond. *Theranostics* **2024**, *14*, 6726.
- 11. Lu, C.; Li, Z.; Wu, N.; et al. Tumor Microenvironment-Tailored Nanoplatform for Companion Diagnostic Applications of Precise Cancer Therapy. *Chem* **2023**, *9*, 3185–3211.
- 12. Jin, Z.; Al Amili, M.; Guo, S. Tumor Microenvironment-Responsive Drug Delivery Based on Polymeric Micelles for Precision Cancer Therapy: Strategies and Prospects. *Biomedicines* **2024**, *12*, 417.
- 13. Shah, D.D.; Chorawala, M.R.; Raghani, N.R.; et al. Tumor Microenvironment: Recent Advances in Understanding and Its Role in Modulating Cancer Therapies. *Med. Oncol.* **2025**, *42*, 1–32.
- 14. Vitorakis, N.; Gargalionis, A.N.; Papavassiliou, K.A.; et al. Precision Targeting Strategies in Pancreatic Cancer: The Role of Tumor Microenvironment. *Cancers* **2024**, *16*, 2876.
- 15. Goenka, A.; Khan, F.; Verma, B.; et al. Tumor Microenvironment Signaling and Therapeutics in Cancer Progression. *Cancer Commun.* **2023**, *43*, 525–561.
- 16. Wu, Q.; Hu, Y.; Yu, B.; et al. Polysaccharide-Based Tumor Microenvironment-Responsive Drug Delivery Systems for Cancer Therapy. *J. Control. Release* **2023**, *362*, 19–43.
- 17. Jiang, L.; Qi, Y.; Yang, L.; et al. Remodeling the Tumor Immune Microenvironment via siRNA Therapy for Precision Cancer Treatment. *Asian J. Pharm. Sci.* **2023**, *18*, 100852.
- 18. Lee, R.Y.; Wu, Y.; Goh, D.; et al. Application of Artificial Intelligence to In Vitro Tumor Modeling and Characterization of the Tumor Microenvironment. *Adv. Healthc. Mater.* **2023**, *12*, 2202457.
- 19. Xie, T.; Huang, A.; Yan, H.; et al. Artificial Intelligence: Illuminating the Depths of the Tumor Microenvironment. *J. Transl. Med.* **2024**, *22*, 799.
- 20. Lin, G.; Wang, X.; Ye, H.; et al. Radiomic Models Predict Tumor Microenvironment Using Artificial Intelligence—The Novel Biomarkers in Breast Cancer Immune Microenvironment. *Technol. Cancer Res. Treat.* **2023**, *22*, 15330338231218227.
- 21. DuCote, T.J.; Naughton, K.J.; Skaggs, E.M.; et al. Using Artificial Intelligence to Identify Tumor Microenvironment Heterogeneity in Non–Small Cell Lung Cancers. *Lab. Investig.* **2023**, *103*, 100176.
- 22. Lobanova, O.A.; Kolesnikova, A.O.; Ponomareva, V.A.; et al. Artificial Intelligence (AI) for Tumor Microenvironment (TME) and Tumor Budding (TB) Identification in Colorectal Cancer (CRC) Patients: A Systematic Review. *J. Pathol. Inform.* **2024**, *15*, 100353.
- 23. Feng, S.; Yin, X.; Shen, Y. Artificial Intelligence-Powered Precision: Unveiling the Tumor Microenvironment for a New Frontier in Personalized Cancer Therapy. *Intell. Med.* **2025**, *5*, 95–98.
- 24. Samani, Z.R.; Parker, D.; Akbari, H.; et al. Artificial Intelligence-Based Locoregional Markers of Brain Peritumoral Microenvironment. *Sci. Rep.* **2023**, *13*, 963.
- 25. Ye, Y.; Wu, X.; Wang, H.; et al. Artificial Intelligence-Assisted Analysis for Tumor-Immune Interaction Within the Invasive Margin of Colorectal Cancer. *Ann. Med.* **2023**, *55*, 2215541.
- 26. Zhou, T.; Man, Q.; Li, X.; et al. Artificial Intelligence-Based Comprehensive Analysis of Immune-Stemness-Tumor Budding Profile to Predict Survival of Patients With Pancreatic Adenocarcinoma. *Cancer Biol. Med.* **2023**, *20*, 196–217.
- 27. Li, J.; Li, L.; You, P.; et al. Towards Artificial Intelligence to Multi-Omics Characterization of Tumor Heterogeneity in Esophageal Cancer. *Semin. Cancer Biol.* **2023**, *91*, 35–49.
- 28. Feng, Z.; Lin, H.; Liu, Z.; et al. Artificial Intelligence-Quantified Tumour-Lymphocyte Spatial Interaction Predicts Disease-Free Survival in Resected Lung Adenocarcinoma: A Graph-Based, Multicentre Study. *Comput. Methods Programs Biomed.* **2023**, *238*, 107617.



Publisher's Note: The views, opinions, and information presented in all publications are the sole responsibility of the respective authors and contributors, and do not necessarily reflect the views of UK Scientific Publishing Limited and/or its editors. UK Scientific Publishing Limited and/or its editors hereby disclaim any liability for any harm or damage to individuals or property arising from the implementation of ideas, methods, instructions, or products mentioned in the content.